HORSEHOE VORTICES IN UNIFORMLY SHEARED TURBULENCE

Christina Vanderwel
Department of Mechanical Engineering
University of Ottawa
Ottawa, Ontario, Canada
cvand072@uottawa.ca

Stavros Tavoularis
Department of Mechanical Engineering
University of Ottawa
Ottawa, Ontario, Canada
stavros.tavoularis@uottawa.ca

ABSTRACT

Uniformly sheared flow (USF) with a turbulence Reynolds number Re_λ of approximately 150 and a shear rate parameter of approximately 12 has been generated in a water tunnel and its instantaneous structure has been examined using flow visualization, laser Doppler velocimetry and particle image velocimetry. Horseshoe-shaped vortices, similar to those observed in turbulent boundary layers (TBL), were found to be prevalent in this flow. These vortices were observed within relatively strong shear layers, which separated regions of fluid with nearly uniform velocity. Like TBL, USF was found to contain structures whose heads pointed towards the high speeds, but, in contrast to TBL, USF also contained inverted structures. These results demonstrate that organized horseshoe/hairpin-type vortices are generated by mean shear irrespectively of the presence of solid walls.

INTRODUCTION

The characteristics of coherent structures in turbulent boundary layers (TBL) have been documented by many researchers both experimentally and through direct numerical simulations (DNS). Earlier experimental studies were based largely on flow visualisation using hydrogen bubbles, dyes, or smoke (e.g., Kline et al., 1967; Head and Bandyopadhyay, 1981), but more recently many studies used particle image velocimetry (PIV) to obtain instantaneous velocity maps of the flow (e.g., Meinhart and Adrian, 1995; Adrian, Meinhart, and Tomkins, 2000; Gao, Ortiz-Duenas, and Longmire, 2007). Examples of DNS of coherent structures in the TBL include the work by Zhou et al. (1999) and Wu and Moin (2009). All these studies have identified the same type of dominant coherent structures, similar to the one sketched in figure 1. Such structures are referred to as horseshoe vortices by some authors and as hairpin vortices by others. Horseshoe vortices in TBL always appear with their heads pointing downstream and away from the wall, namely towards the high-velocity fluid. They have been observed to form and travel in groups, in a way that their combined effect is to create local zones of low momentum fluid, as illustrated in figure 1 (Meinhart and Adrian, 1995). Horseshoe/hairpin vortices make a major contribution to the turbulent stresses and turbulent transport (Adrian, 2007). In TBL, the generation of both the mean shear and the horseshoe vortices are attributed to the solid wall. Nevertheless, DNS (Rogers and Moin, 1987; Lee, Kim, and Moin, 1990) have demonstrated that horseshoe vortices are also present in temporally evolving homogeneous shear flow (HSF), which is free of solid walls. Horseshoe vortices in HSF

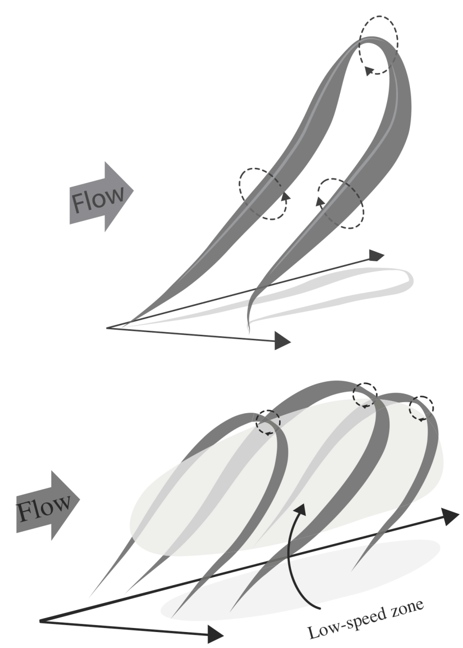

Figure 1: Sketches of a typical horseshoe vortex (top) and a group of aligned horseshoe vortices (bottom).

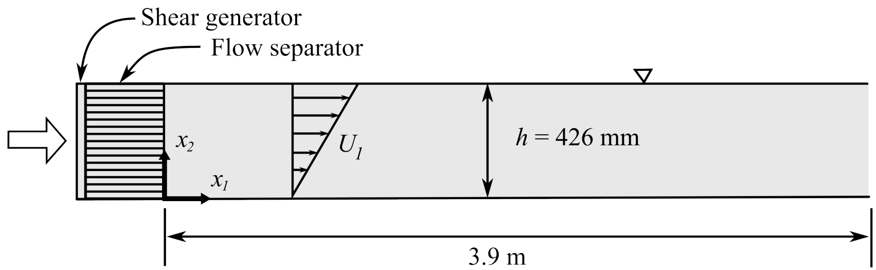

Figure 2: Schematic diagram of the experimental setup.

were observed to have heads pointing towards either the high- or the low-speed fluid (Rogers and Moin, 1987). Qualitative experiments by Kislich-Lemyre (2002) have indicated that horseshoe vortices also appear in uniformly sheared flows (USF), in which the turbulence is stationary, transversely homogeneous, evolving streamwise and nearly free of wall effects. The objectives of this work are to document qualitatively and quantitatively the characteristic properties of coherent structures appearing in USF and to compare them with the properties of coherent structures in TBL.

FLOW APPARATUS AND INSTRUMENTATION

All experiments were conducted in a recirculating water channel, having a test section that was 0.54 m wide, 3.9 m long, and filled with water to a depth of 0.426 m (see figure 2). Uniform mean shear was generated by a perforated plate having a solidity that varied linearly in the vertical direction; it was followed by a flow separator, consisting of a set of parallel channels, which straightened the mean stream and established a nearly uniform initial integral length scale of turbulence.

A two-component laser Doppler velocimeter (LDV) was used for measuring the time-averaged statistics of the flow. The flow patterns were investigated using conventional hydrogen bubble and fluorescent dye flow visualisation methods as well as a novel scanning dye visualisation method, in which patterns of fluorescent dye at multiple cross-sections in the flow were illuminated by rapidly scanning the flow with a laser light sheet and recorded by a high-speed camera. Instantaneous velocity maps were obtained by a 2D particle image velocimetry (PIV) system at a maximum rate of 7.24 frames/s. Particles images had a resolution of 2048×2048 pixels and were processed to produce a vector field of 128×128 vectors, covering a field of view of 100×100 mm.

RESULTS

Time-averaged flow properties

The time-averaged centreline velocity was U_c = 0.16 m/s and the mean shear was $d\bar{U}_1/dx_2$ = 0.45 s^{-1}. The streamwise evolution of the turbulence was expressed in terms of the dimensionless development time (also signifying the total mean strain) defined as

$$\tau = \int_0^{x_1} \frac{1}{U_c}\frac{d\bar{U}_1}{dx_2}dx_1 \tag{1}$$

The turbulence structure was deemed to be fully developed and approximately transversely homogeneous in the region $5 < \tau < 9$, which occupied the downstream half of the test section. At $\tau = 5$, the integral length scale was L_{11} = 0.027 m, the turbulence Reynolds number was Re_λ = 150 and the shear rate parameter, defined as

$$S^* = \frac{2k}{\varepsilon}\frac{d\bar{U}_1}{dx_2} \tag{2}$$

was approximately 12; in this equation, k is the kinetic energy per unit mass and ε is the kinetic energy dissipation rate per unit mass. The streamwise distance over which a typical eddy would be convected during its lifetime, defined as

$$L_e = U_c\frac{2k}{\varepsilon} \tag{3}$$

was approximately 4.4 m. The Reynolds stress anisotropy tensor and other normalized statistical properties were comparable to those measured in previous USF experiments with comparable S^* (Tavoularis and Karnik, 1989).

Flow Visualisation Using a Fluorescent Dye

Fluorescent dye patterns in the flow were illuminated using a laser sheet and recorded by a camera positioned such as to record images on the plane of the light sheet. As shown in figure 3, the light sheet was inclined by 45° with respect to the flow direction and illuminated the cross-sections of vortices with axes that were roughly perpendicular to the light plane. As illustrated in figure 4, which contains hand-drawn sketches superimposed on the photograph, the recorded images contained many mushroom-shaped dye patterns having diverse orientations. Each of these patterns was interpreted to mark the legs of a horseshoe vortex (see discussion by Head and Bandyopadhyay, 1981). Upright and inverted mushroom-shaped dye patterns correspond to upright and inverted horseshoe vortices, respectively. Some variation from these two exact orientations is apparent in figure 4; this may be attributed to vortex asymmetry or contortions of vortices by the turbulent flow.

The laser sheet was scanned towards the upstream at a speed of approximately 1 m/s, completing the scan in less than 1 s, making it possible to record effectively `frozen', three-

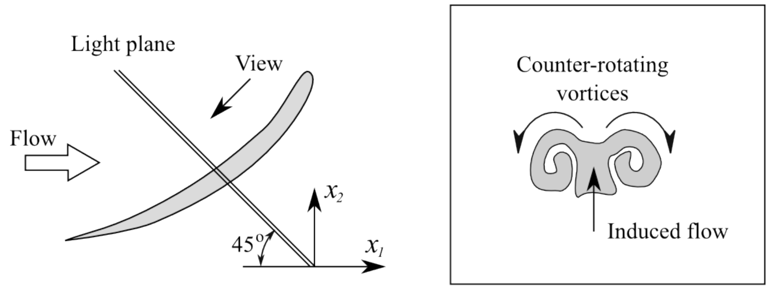

(a) (b)

Figure 3: Sketches of the dye visualisation setup (adapted from Head and Bandyopadhyay, 1981): (a) side view perpendicular to the light plane, and (b) visualised cross-section of a horseshoe vortex in the form of a mushroom-shaped dye pattern.

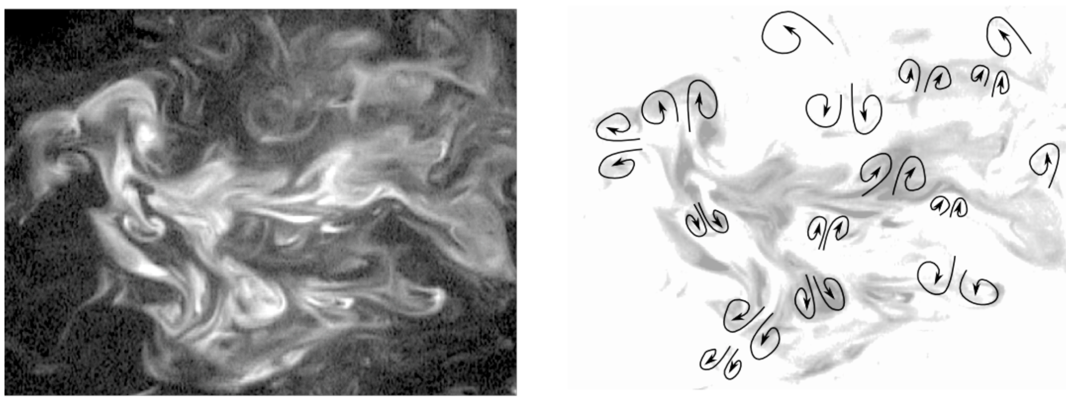

(a) (b)

Figure 4: Typical dye patterns; (a) photograph of the flow; (b) hand-drawn mushroom-shaped patterns with diverse orientations.

dimensional flow patterns. Images were recorded at a rate of 500 frames per second, resulting in an average spacing of 3 mm between images, which is equal to approximately 0.11 L_{11} or 0.0007 L_e. These scans determined that the mushroom-shaped dye patterns were coherent over streamwise distances of typically about 2 L_{11}; this distance is deemed to be the typical streamwise length of the horseshoe vortices in the flow.

Flow Visualisation Using Hydrogen Bubbles

Hydrogen bubbles were released in the form of timelines from a thin wire placed in the middle of the test section. Timelines released from a horizontal wire were observed to deform into horseshoe-like shapes, as shown in figure 5. The legs of the horseshoes were traced across several timelines following the quasi-streamwise alignment of line segments; the heads of the structures were clearly visible in the bubble patterns in the form of arches connecting two elongated legs. The horseshoe vortices in the USF were both forward-facing and backward-facing, corresponding to upright and inverted structures, in contrast to those in TBL which are only upright. As the structures travelled downstream, they were stretched along a plane that was inclined by approximately 45˚, until the bubble lines became very thin and they could no longer be identified. The length of the structures varied from 1.5 L_{11} to 3 L_{11}, and the distance between the legs was comparable to L_{11}.

Timelines released from a vertical wire (figure 6) became tilted with time, as the bubbles introduced at a relatively high elevation were generally convected downstream faster than those at lower elevations. As they moved downstream, these timelines also became distorted, thus revealing the strongly non-linear shapes of instantaneous velocity profiles, which contrast sharply the linear shape of the time-averaged velocity profile. Bubble patterns also reveal the frequent presence of strong clockwise vortices, which are interpreted to be the cross-sections of heads of horseshoe-vortices.

PIV Measurements

Instantaneous velocity vector fields on selected planes were reconstructed from PIV measurements. In a vertical plane (figure 7), the vertical velocity gradient appears to be composed of uniform-velocity zones separated by strong shear layers, comparable to observations of the vertical bubble

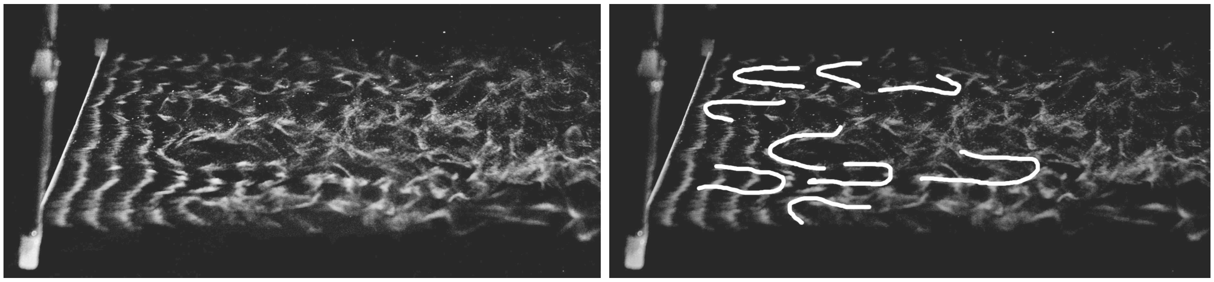

(a) (b)

Figure 5: Images of hydrogen bubbles released from a horizontal line source; (a) photograph of the flow; (b) hand-drawn lines connecting bubbles from different timelines, which identify the presence of horseshoe-shaped patterns.

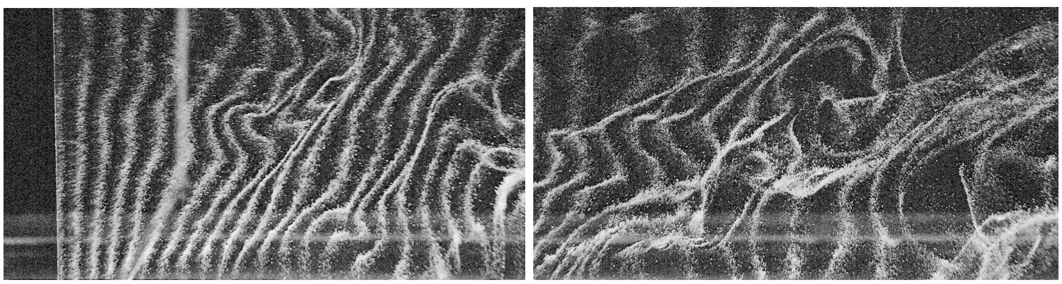

(a) (b)

Figure 6: Images of hydrogen bubbles released from a vertical line source; (a) timelines near the bubble source, which become slanted as a result of the vertical velocity variation but also illustrate the presence of roller vortices; (b) timelines away from the source, which clearly depict strong roller vortices.

timelines. The instantaneous velocity profile (solid line) in figure 7, which corresponds to the middle of the contour plot, is step-wise, and therefore distinctly non-uniform, in contrast to the uniform time-averaged velocity profile (dashed line). Vortices were identified at locations at which the swirling strength had local peaks with $\lambda > 0.05\lambda_{max}$, where λ_{max} was the maximum swirling strength in the flow map. Vortices were found to congregate along the shear layers that divided the zones of uniform velocity. Clockwise vortices were much more numerous than counter-clockwise ones and were construed to be the cross-sections of horseshoe vortex heads. These observations are similar to those from TBL studies (e.g., Adrian, 2007).

In a horizontal plane (figure 8), cross-sections of the vortex legs were identified as pairs of counter-rotating vortices, travelling side-by-side, while accompanied by streaks of low- or high-speed fluid between them. Vortex pairs that were associated with a low-speed region of flow are deemed to be the legs of upright horseshoe vortices, whereas vortex pairs that were associated with a high-speed region of flow correspond to the legs of inverted horseshoe vortices. The dimensions of the horseshoe vortices identified from PIV measurements were comparable to their estimates using the other measurement techniques.

DISCUSSION

All experimental methods used in the present USF study confirmed the abundance of horseshoe vortices with typical streamwise lengths of up to 3 L_{11} and typical widths of about L_{11}. Our observations indicated that both upright and inverted horseshoe vortices are prevalent in USF. The inverted structures appear to have legs inclined at the same angle as the upright structures; however, these legs are connected at the upstream, lower end rather than the downstream, upper end. The vortex filament that comprises the inverted structure rotates such that fluid is induced downwards and downstream between the legs. Inverted horseshoe vortices have not been observed in TBL but were previously found to exist in HSF by Rogers and Moin (1987) using DNS.

We postulate that the mechanism of horseshoe vortex formation in USF is similar to that in TBLs, as described by Smith et al. (1991) and Davidson (2004). In both cases, the unperturbed mean flow may be viewed as consisting of sheets of quasi-two-dimensional spanwise vortices. In the presence of a disturbance, these vortex filaments stretch in the direction of mean strain and form horseshoe vortices. We hypothesize that unbounded shear tends to produce both upright and inverted structures equally, however, the obstruction by the wall in TBL suppresses the formation of inverted structures. This observation separates the effects of the mean shear from

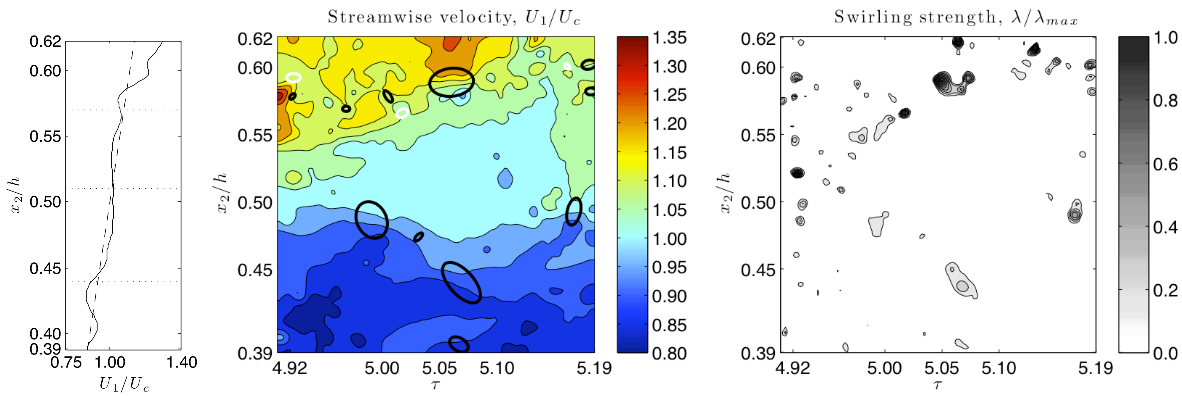

Figure 7: Instantaneous velocity profile (left) and contours of velocity (centre) and swirling strength (right) obtained from PIV measurements in a vertical plane containing the streamwise direction. Ellipses superimposed on the velocity map mark the locations of clockwise vortices identified as peaks in swirling strength; black ellipses indicate clockwise rotation, whereas white ellipses are counter-clockwise. Clockwise vortices are interpreted as the cross-sections of the heads of horseshoe vortices.

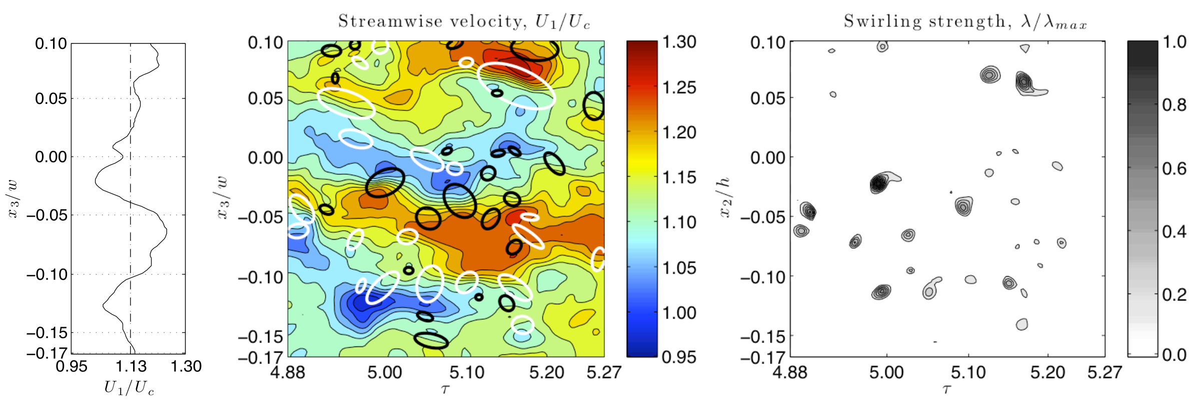

Figure 8: Instantaneous velocity profile (left) and contours of velocity (centre) and swirling strength (right) obtained from PIV measurements in a horizontal plane. Ellipses superimposed on the velocity map mark the locations of clockwise vortices identified as peaks in swirling strength; black ellipses indicate clockwise rotation, whereas white ellipses are counter-clockwise. Counter-rotating vortices appear to bestride low- and high-speed streamwise streaks.

the combined effects of a solid wall. This mechanism is illustrated in figure 9.

These results further support the hypothesis (Rogers & Moin, 1987; Lee et al., 1990) that mean shear, irrespective of the presence of a wall, is sufficient to generate horseshoe structures.

CONCLUSIONS

This research is the first to quantitatively document the presence of horseshoe-shaped vortices in USF using experimental methods. All evidence collected by three different measurement techniques supports the hypothesis that horseshoe vortices are prevalent in USF, having a similar shape to those observed in TBL. The quintessential horseshoe vortex of the USF is inclined upwards from the streamwise direction, stretches up to 3 L_{11} in the streamwise direction, and its legs are spaced by about L_{11}. However, in contrast to those in TBL, horseshoes in USF were observed to span a wide range of orientations, and included inverted as well as upright structures. It is hypothesized that the presence of the wall in the TBL acts to suppress the development of inverted structures, whereas this effect is not present in USF. These results indicate that free shear, without a wall, is sufficient to form horseshoe structures, and that the wall acts to reorganise the structures and restrict their orientations.

Financial support by Le Fonds Québécois de la Recherche and by the Natural Sciences and Engineering Research Council of Canada (NSERC) is gratefully acknowledged.

REFERENCES

R. J. Adrian, “Hairpin vortex organization in wall turbulence,” Physics of Fluids, vol. 19, no. 4, p. 041301, 2007.

R. J. Adrian, C. D. Meinhart, and C. D. Tomkins, “Vortex organization in the outer region of the turbulent

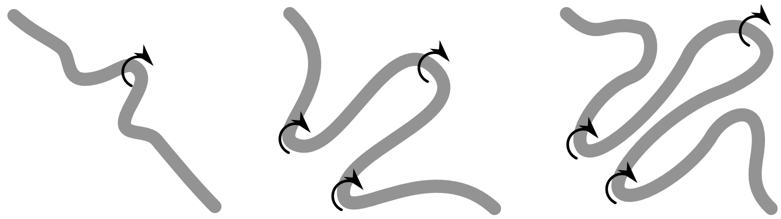

Figure 9: A scenario for the generation of horseshoe vortices as evolutions of quasi-two-dimensional spanwise vortex filaments. In the presence of a disturbance, these vortex filaments stretch in the direction of mean strain and form both upright and inverted horseshoe vortices. This image is reminiscent of figures presented by Smith et al. (1991) and Robinson (1991) in their discussion of the formation of symmetric hairpin vortices, although, these references do not discuss the potential for generation of inverted hairpins.

boundary layer," Journal of Fluid Mechanics, vol. 422, pp. 1–54, Nov. 2000.

Q. Gao, C. Ortiz-Duenas, and E. K. Longmire, "Circulation signature of vortical structures in turbulent boundary layers," in 16th Australasian Fluid Mechanics Conference (AFMC) (P. Jacobs, T. McIntyre, M. Cleary, D. Buttsworth, D. Mee, R. Clements, R. Morgan, and C. Lemckert, eds.), (Brisbane, Australia), pp. 135–141, School of Engineering, The University of Queensland, December 2007.

M. R. Head and P. Bandyopadhyay, "New aspects of turbulent boundary-layer structure," Journal of Fluid Mechanics, vol. 107, pp. 297–338, 1981.

B. Kislich-Lemyre, The large-scale structure of uniformly sheared turbulence and its distortion by a solid wall at rest or in motion. PhD Dissertation, Department of Mechanical Engineering, University of Ottawa, July 2002.

S. Kline, W. Reynolds, F. Schraub, and P. Runstadler, "The structure of turbulent boundary layers," Journal of Fluid Mechanics, vol. 30, no. 04, pp. 741–773, 1967.

M. J. Lee, J. Kim, and P. Moin, "Structure of turbulence at high shear rate," Journal of Fluid Mechanics, vol. 216, pp. 561–583, June 1990.

C. Meinhart and R. Adrian, "On the existence of uniform momentum zones in a turbulent boundary layer," Physics of Fluids, vol. 7, no. 4, pp. 694–696, 1995.

S. K. Robinson, "Coherent motions in the turbulent boundary layer," Annual Review of Fluid Mechanics, vol. 23, pp. 601-639, 1991.

M. M. Rogers and P. Moin, "The structure of the Vorticity field in homogeneous turbulent flows," Journal of Fluid Mechanics, vol. 176, pp. 33–66, 1987.

C. R. Smith, J. D. A. Walker, A. H. Haidari, and U. Sobrun, "On the Dynamics of Near-Wall Turbulence," Philosophical Transactions: Physical Sciences and Engineering, vol. 336, No. 1641, pp. 131-175, 1991.

S. Tavoularis and U. Karnik, "Further experiments on the evolution of turbulent stresses and scales in uniformly sheared turbulence," Journal of Fluid Mechanics, vol. 204, pp. 457–478, 1989.

X.Wu and P. Moin, "Direct numerical simulation of turbulence in a nominally zero-pressure-gradient flat-plate boundary layer," Journal of Fluid Mechanics, vol. 630, pp. 5–41, 2009.

J. Zhou, R. J. Adrian, S. Balachandar, and T. M. Kendall, "Mechanisms for generating coherent packets of hairpin vortices in channel flow," Journal of Fluid Mechanics, vol. 387, pp. 353–396, May 1999.